JOTCS A
Journal of the Turkish Chemical Society
Section: A
Chemistry
TURKISH CHEMICAL SOCIETY

Removal of Cu(II), Ni(II), and Cd(II) Ions from Aqueous Media using Glycidyl Methacrylate-Grafted Poly(ethylene terephthalate) Fibers Functionalized with Hydroxyl Amine

Yılmaz Mert[1]*, Mustafa Yiğitoğlu[2], Zülfikar Temoçin[1], Osman Çaylak[3]

[1]Department of Chemistry, Faculty of Engineering and Natural Sciences, Kırıkkale University, Yahsihan, 71450, Kirikkale, Türkiye.
[2]Department of Bioengineering, Faculty of Engineering and Natural Sciences, Kırıkkale University, Yahsihan, 71450, Kirikkale, Türkiye.
[3]Vocational School of Health Services, Department of Pharmacy, Sivas Cumhuriyet University, Türkiye.

Abstract: In this study, poly(ethylene terephthalate) (PET) fiber was treated with glycidyl methacrylate (GMA) using benzoyl peroxide (Bz_2O_2) to start the reaction in water (GMA-g-PET). Then, hydroxylamine (HA) was chemically attached to the GMA-treated PET fiber (HA-GMA-g-PET). The results indicated that a nitrogen atom was connected to 95% of the GMA-treated PET fiber at a rate of 5.99%, with the reaction happening at a temperature of 75 °C for 75 min. Hydroxylamine (HA) was then covalently attached to the GMA-grafted PET fiber (HA-GMA-g-PET). The results showed that 95% of the GMA-grafted PET fiber had a nitrogen atom attached at a rate of 5.99%, with the reaction taking place at 75 °C for 75 min. The removal of Cu(II), Ni(II), and Cd(II) ions from the aqueous solution by the HA-GMA-g-PET fiber was examined by the batch equilibration technique. Researchers investigated how parameters such as pH, adsorption temperature, adsorption time, and initial ion concentration affect the adsorption capacity of HA-GMA-g-PET fibers. The maximum adsorption capacities of the reactive fiber at a concentration of 300 mg/L for Cu(II), Ni(II), and Cd(II) ions at a pH value of 6 were found to be 27.76 mg/g, 63.86 mg/g, and 66.73 mg/g, respectively. It was determined that the adsorption of Cu(II), Ni(II), and Cd(II) ions onto HA-GMA-g-PET fiber attained equilibrium at 90 min, 45 min, and 120 min, respectively. It was observed that at a pH value of 6, HA-GMA-g-PET fiber is more selective for Cd(II) ions in the mixtures of Cu(II)-Cd(II), Ni(II)-Cd(II), and Cu(II)-Ni(II)-Cd(II).

Keywords: Poly(ethylene terephthalate) fibers, Grafting, Adsorption, Heavy metal ions, Hydroxylamine.

Submitted: August 1, 2025. **Accepted:** December 10, 2025.

Cite this: Mert Y, Yiğitoğlu M, Temoçin Z, Çaylak O. Synthesis of Dithizone (DHZ) Removal of Cu(II), Ni(II), and Cd(II) Ions from Aqueous Media using Glycidyl Methacrylate-Grafted Poly(ethylene terephthalate) Fibers Functionalized with Hydroxyl Amine. JOTCSA. 2026, **1756217**, 1-14.

DOI: https://doi.org/10.18596/jotcsa.1756217

***Corresponding author's E-mail:** yilmaz.mert@sivas.edu.tr

1. INTRODUCTION

Heavy metals (HMs) are a significant group of pollutants that endanger the ecological balance due to their toxicity, ability to accumulate in water, soil, and living organisms, and their nondegradable nature (1). HM pollution significantly impacts various ecosystems by degrading soil and water quality, disrupting the ecological balance. Studies have shown that HMs can cause significant pollution and ecological hazards in aquatic environments (2). Ecological risk assessments identified sites with moderate to high HM pollution levels, highlighting the need for remedial actions (2). HMs also affect wastewater treatment systems, leading to difficulties such as the discharge of inadequately treated wastewater and the accumulation of metal levels in sludge, which pose risks to human and environmental health (3). Aquatic organisms absorb pollutants directly from water and indirectly through food chains. HMs have profound effects on fish and other aquatic organisms, including reduced developmental growth, increased developmental anomalies, and the extinction of fish populations in polluted reservoirs. Therefore, greater attention to bio conservation protocols is essential (4). The processes of industrialization and urbanization have precipitated a swift escalation in heavy metal

pollution levels. This pollution has led to the contamination of sediments, soils, and water bodies, thereby increasing the ecological risks associated with these hazardous substances (5). The evaluation of heavy metal contamination in impacted regions depends significantly on comprehending the distribution, origins, interactions, and environmental variables related to it. These elements are essential in determining the possible ecological repercussions (6).

Employing advanced treatment methods is crucial for improving wastewater quality by efficiently removing pollutants that are resistant to standard processes. Various methods, such as advanced oxidation processes (AOPs), membrane separation techniques, electrochemical oxidation, adsorption, and electrocoagulation, are employed for this purpose (7). Despite activated carbon's efficacy as an adsorbent for the extraction of metal ions from aqueous solutions, its prohibitive cost has prompted researchers to seek more economical alternatives. The adsorbents examined for this purpose encompass diverse industrial byproducts, including ash, sludge, lignin, and agricultural residues such as tree bark, bananas, rice husks, peanut shells, and various plant leaves and stems (8,9).

This study involves the grafting of glycidyl methacrylate (GMA) onto PET fibers to create a novel adsorbent. The aim is to covalently attach hyaluronic acid (HA) to the grafted PET fibers through the epoxy groups in the GMA structure. The newly synthesized adsorbent will undergo characterization through scanning electron microscopy (SEM), Fourier transform infrared spectroscopy (FTIR), and thermogravimetric analysis (TGA). Cu(II), Ni(II), and Cd(II) ions have been chosen as model adsorbates to assess their adsorption characteristics. The impact of different operational parameters on the adsorption of these ions will be examined.

2. EXPERIMENTAL SECTION

2.1. Equipment

An Analyst Perkin Elmer 400 atomic absorption spectrometer (Perkin Elmer, Norwalk, CT, USA) equipped with a hollow cathode lamp and an air-acetylene burner was used to determine Cu(II), Ni(II), and Cd(II) ions. When using the devices, the necessary parameters were set in accordance with the manufacturer's recommendations. The selected wavelengths for Cu, Ni, and Cd were 324.8, 232.0, and 228.8 nm, respectively. pH measurements were made using the Hanna HI 221 pH meter (HANNA pH 211, Hanna Instruments, Italy). The shaking of the working solutions was performed using a Medline BS-21 orbital shaker (BS-21, Medline, Hwaseong, Korea). Infrared (IR) spectra were recorded from 400 to 4000 cm^{-1} using an IR spectrophotometer, Bruker VERTEX 70 FT-IR (Bruker Inc., Germany). Thermogravimetric (TGA) analyses were recorded in flowing nitrogen from 25°C to 900°C with a heating rate of 20°C min^{-1} using the high-resolution mode of the TGA-Q500 instrument (TGA Q 500, TA Instruments, USA). SEM measurements were carried out with a JSM 5600 model scanning electron microscope (JSM-5600, JEOL, Tokyo, Japan).

2.2. Chemicals and Reagents

Polyethylene terephthalate (PET) fibers were provided by SASA (Artificial and Synthetic Fiber Inc., Adana, Turkey). Glycidyl methacrylate (GMA, 97.0%) was obtained from SRL Chemicals in Mumbai, India. Benzoyl peroxide (Bz_2O_2, pure grade), copper(II) nitrate trihydrate ($Cu(NO_3)_2.3H_2O$, 99.5%), nickel(II) nitrate hexahydrate ($Ni(NO_3)_2.6H_2O$, 99.9%), cadmium(II) nitrate tetrahydrate ($Cd(NO_3)_2.4H_2O$, ≥98.5%), acetone (99.7%), sodium acetate trihydrate ($CH_3COONa.3H_2O$, 99.5%), glacial acetic acid (CH_3COOH, 99.9%), sodium dihydrogen phosphate (NaH_2PO_4, ≥99%), phosphoric acid (H_3PO_4, 99%), nitric acid (HNO_3, 65%), and sodium hydroxide (NaOH, 97.0%) were procured from Merck (Darmstadt, Germany). A 50 wt% hydroxylamine solution in H_2O (99.999%) was obtained from Sigma-Aldrich. All solution preparations utilized ultrapure water generated by a BIO-AGE Direct Ultra (TUVF-5) Water Purifier System.

2.3. Polymerization Procedure

GMA-g-PET fiber was synthesized according to the literature (10). Briefly, 300 mg of PET fibers were placed in 50 mL of dichloroethane at 90°C for 2 h. The swollen fibers were placed on filter paper to remove dichloroethane and were taken into the polymerization tube. 2 mL of acetone solution containing the required amount of GMA and appropriate concentration of Bz_2O_2 was added to the tube, and the volume was completed to 20 mL with distilled water. The polymerization tube was kept in a water bath at 75°C for 2 hours to complete the polymerization. The grafted fiber was cleaned with acetone for 24 hours and left to dry at 50°C for 3 days. Using the weight increase in the grafted fiber, graft yield (GY) was calculated with equation 1.

$$GY\% = \frac{(w_g - w_i)}{w_i} \times 100 \quad (1)$$

The weight of ungrafted fibers is represented by w_i, while the weight of grafted fibers is represented by w_g.

2.4. Preparation of the HA-GMA-g-PET Fiber

0.05 g of GMA-g-PET fiber was taken into a 50 mL Erlenmeyer flask, and 5 mL of 50% HA was added. This mixture was shaken in an orbital shaker at 125 rpm for 75 min at 75 °C. The synthesis reaction is shown in Figure 1.

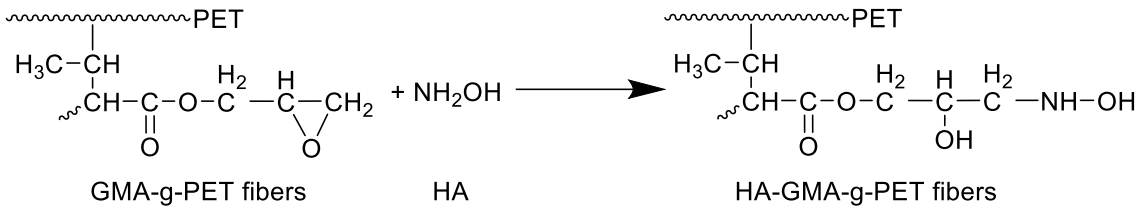

Figure 1: Synthesis reaction of HA-GMA-g-PET fiber.

2.5. Adsorption Procedure

Adsorption was carried out using a batch process in 50 mL Erlenmeyer flasks. Approximately 0.05 g of HA-GMA-g-PET fiber was mixed with 25 mL of metal solution at 125 rpm under specific temperature, pH, and time conditions. Samples were taken at specific intervals, and the metal ion concentration was determined using AAS. The results were presented by calculating the amount of metal adsorbed per gram of HA-GMA-g-PET fiber. The adsorbed metal ion was calculated using the following equation.

$$Q = \left[\frac{C_o - C}{m}\right] V \qquad (2)$$

Where Q represents the amount of ions adsorbed by one gram of adsorbent (mg/g), C_o is the initial concentration of the metal solution (mg/L), C is the equilibrium concentration of the metal solution (mg/L), V is the volume of the metal solution (L), and m is the amount of adsorbent (g).

2.6. Desorption of Metal Ions

A batch process was used in desorption studies. Adsorbed metal ions were desorbed with 25 mL of 1 M HNO_3 solution at 25°C. The samples taken from the desorption solutions were analyzed in AAS, and the amount of desorbed metal ions was determined. The desorption percentage was calculated using equation 3.

$$Desorption(\%) = \frac{w_d}{w_a} \times 100 \qquad (3)$$

where w_d is the desorbed ion amount (mg) and w_a is the adsorbent's adsorbed ion amount (mg).

3. RESULTS AND DISCUSSION

3.1. Characterization

3.1.1. FTIR analysis

FTIR spectra of ungrafted PET fibers, GMA-g-PET fibers, and HA-GMA-g-PET fibers are shown in Figure 2. The FTIR fingerprints for ungrafted PET (Figure 2a) were composed of five main peaks at 1713, 1407, 1222, 1100, and 739 cm^{-1}, corresponding to C=O bond stretching in esters, C-H bond stretching, C-O bond stretching in aromatic ether, C-O-C bond stretching in ether, and aromatic C-H stretching (11,12). The peak at 904 cm^{-1} seen because of GMA grafting in the spectrum given in Figure 2b belongs to the asymmetric stretching vibrations of the epoxy functional group. This data showed that GMA was grafted onto PET fiber (13). In the spectrum shown in Figure 2c, the peak at 904 cm^{-1}, which corresponds to the epoxy groups introduced by grafting the GMA monomer onto the PET fiber, disappeared due to a reaction between the amine groups and the epoxy groups. Additionally, in the spectrum given in Figure 2c, O-H absorption at 3270 cm^{-1}, N-H bending vibrations at 1601 cm^{-1} and 1556 cm^{-1}, and C-N stretching vibrations at 1153 cm^{-1} were observed. This data showed that HA is incorporated into the GMA-g-PET structure (14).

3.1.2. SEM analysis

Scanning electron microscope (SEM) photographs of PET fiber and GMA-grafted PET fiber are shown in Figure 3. When the SEM photographs were examined, it was seen that the surface of the ungrafted PET fiber (Figure 3a) was flatter, smoother, and homogeneous. An increase in fiber diameter was observed because of grafting GMA onto PET fiber (Figure 3b). While the diameter of the ungrafted PET fiber was 12.0 μm, the surface of the 95% GMA-grafted PET fiber became heterogeneous and rough, and its diameter was measured as 28.1 μm. These changes in the fiber structure were evidence that GMA was grafted onto PET fiber (15).

3.1.3. TGA analysis

TGA analysis was performed to characterize the new adsorbent obtained because of binding HA to the structure formed by grafting GMA monomer onto PET fiber. The TGA of PET fiber, GMA-g-PET fiber, and HA-GMA-g-PET fiber is shown in Figure 4. While the initial mass loss temperature of ungrafted PET fiber is approximately 400°C, this value is approximately 200°C for GMA-grafted PET fiber. By binding HA to the structure, this value decreased even further at lower temperatures. As clearly seen from the TGA analysis, the introduction of new functional groups to PET fiber chains reduces the mass loss onset temperature.

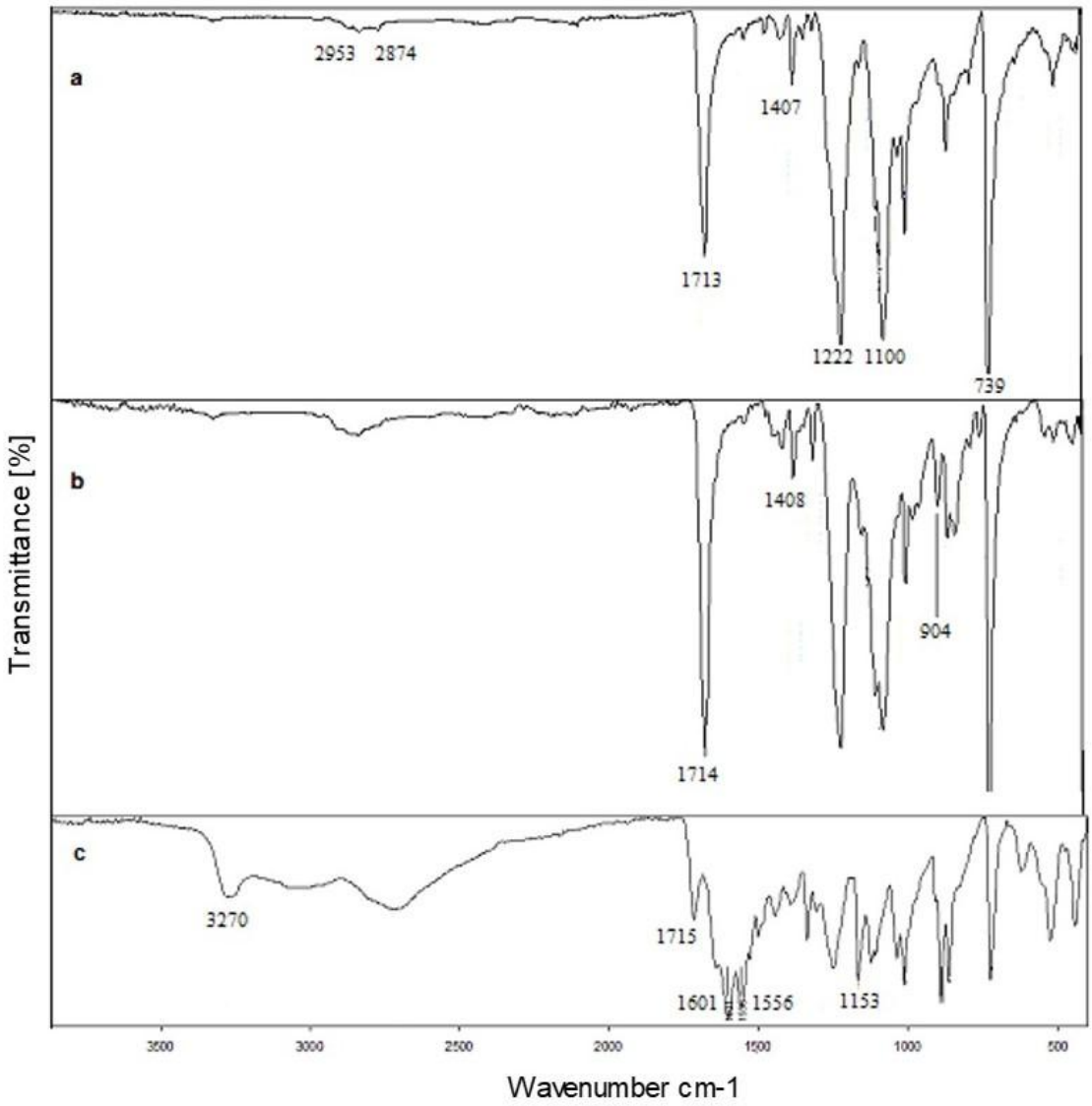

Figure 2: FTIR spectra of (a) PET fibers, (b) GMA-g-PET fibers, and (c) HA-GMA-g-PET fibers.

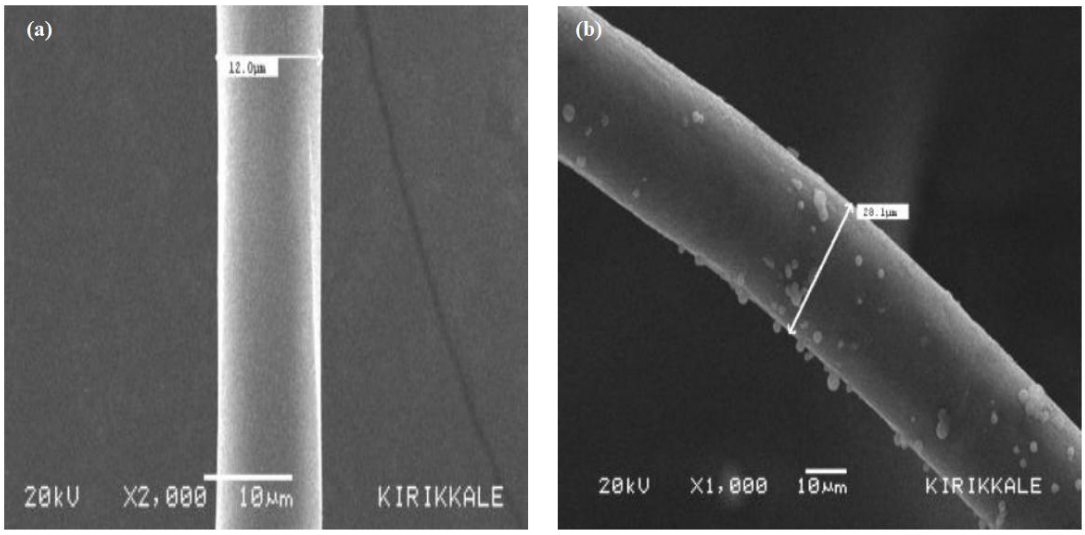

Figure 3: SEM micrographs of (a) PET fibers and (b) GMA-grafted PET fibers (having 95% grafting yield).

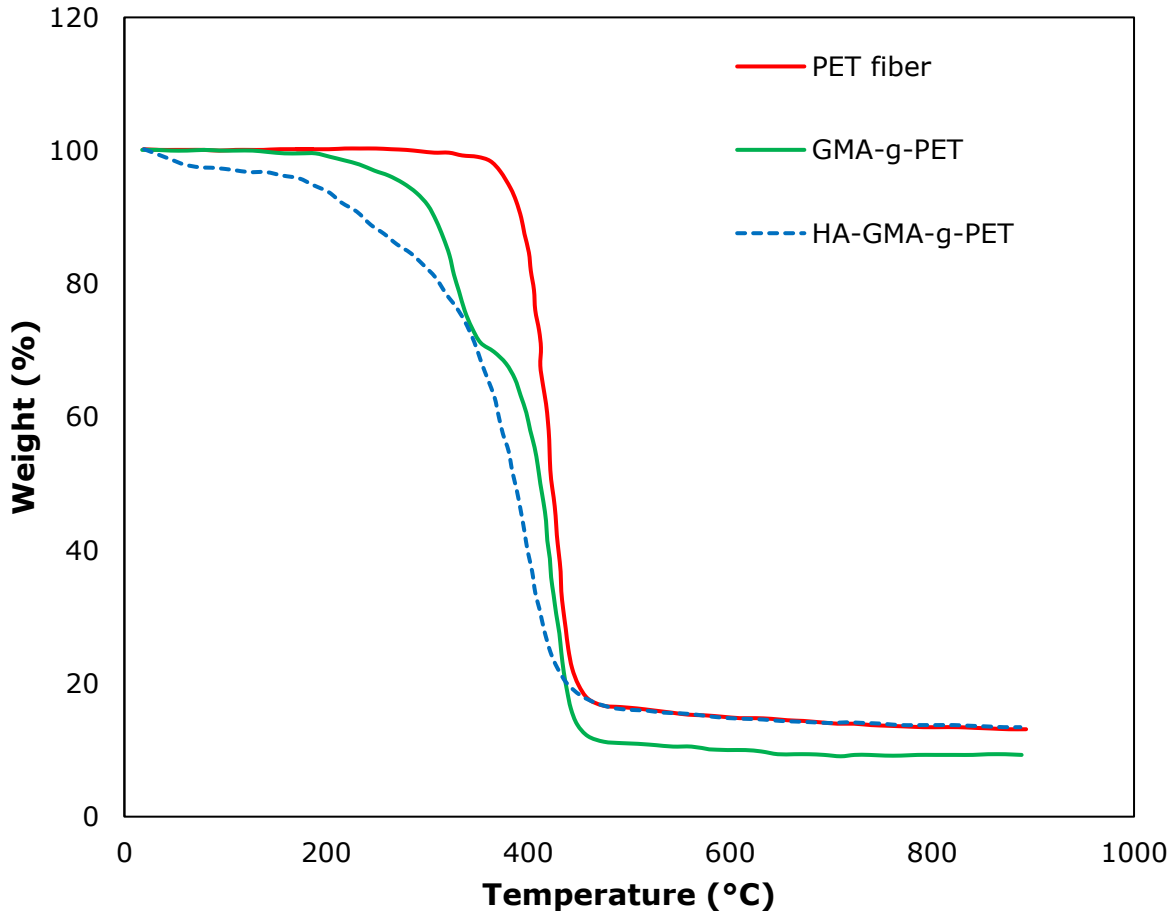

Figure 4: TGA thermograms of PET fibers, GMA-g-PET fiber, and HA-GMA-g-PET fibers.

3.2. Optimization of HA Binding Parameters to GMA-g-PET Fiber

To provide suitable functional groups to GMA-g-PET fibers to be used as adsorbents in the adsorption of heavy metal ions, the fibers were functionalized using HA. The structure formed by covalently bonding HA to the epoxy groups on the PET fiber is shown in Figure 1. Experimental conditions such as temperature, reaction time, and grafting efficiency that affect the binding of HA were investigated. The optimum conditions affecting the binding of HA to GMA-g-PET fibers were determined according to the maximum amount of Cu(II) metal ion adsorbed.

The relationship between the maximum amount of Cu(II) metal ion adsorbed by the HA-GMA-g-PET fiber and the reaction temperature at which HA binds is shown in Figure 5a. As can be seen in the figure, the amount of adsorbed metal ions increases with the binding temperature of HA. This value reached its maximum at 75°C. There was no significant change at higher temperatures. The data obtained show that HA binds to the GMA-g-PET structure at a maximum rate at temperatures of 75°C and above. The elemental analysis results of the amounts of N atoms bound at different temperature values are shown in Figure 5b. Elemental analysis data show that as the temperature increases, the amount of N atoms bonded to the GMA-g-PET structure increases, and accordingly, the amount of HA increases.

3.3. Effects of pH on Adsorption

One of the most important parameters affecting the adsorption behavior of metal ions on the adsorbent is the pH value of the aqueous solution. We examined the effect of pH on the adsorption of metal ions using HA-GMA-g-PET fiber at pH values between 3 and 8 (Figure 6). pH tests were performed below 8 due to the possibility of precipitation of analytes into their hydroxides. Since there are no suitable functional groups to be used in the adsorption of metal ions on GMA-g-PET fiber, metal adsorption is not affected by solution pH values, and metal ion adsorption remains at very low values. As a result of the covalent bonding of HA to the epoxy groups in the GMA structure, the adsorbent was functionalized and obtained a structure suitable for metal adsorption. At low pH values, the high proton concentration in the solution makes the surface of the adsorbent positive by protonating the functional groups (-NH, -OH) on the HA-GMA-g-PET fiber. The degree of adsorption decreases as a result of the repulsion force between Cu(II), Ni(II), and Cd(II) cations and the adsorbent surface. As pH increases, the degree of protonation of active functional groups on the adsorbent surface decreases, while the adsorption amount of analytes increases. The maximum adsorption amounts on HA-GMA-g-PET fiber occurred at pH 5 for Cu(II) ions and at pH 6 for Ni(II) and Cd(II) ions. The formation of hydroxides (16) likely explains the decrease in the adsorption levels of analytes at high pH.

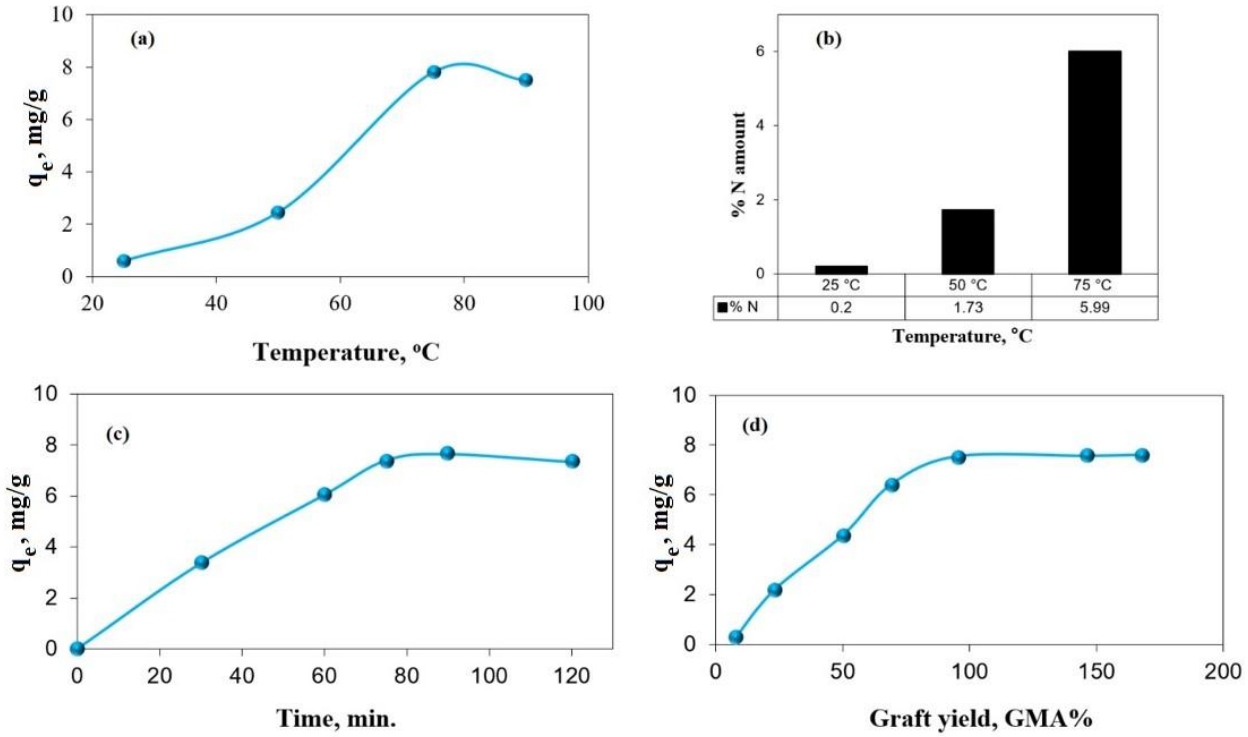

Figure 5: Results of HA binding conditions to GMA-g-PET fibers; **a)** effect of temperature on the functionalization of GMA-g-PET fiber with HA ([Cu(II)]=50 mg/L, pH=5, time=90 min, graft yield=95%), **b)** elemental analysis results of HA-GMA-g-PET fiber structure, **c)** effect of time on the functionalization of GMA-g-PET fiber with HA ([Cu(II)]=50 mg/L, pH=5, temperature=75°C; grafting efficiency=95%); **d)** effect of grafting efficiency on the functionalization of GMA-g-PET fiber with HA ([Cu(II)]=50 mg/L, pH=5, temperature=75°C; time=75 min).

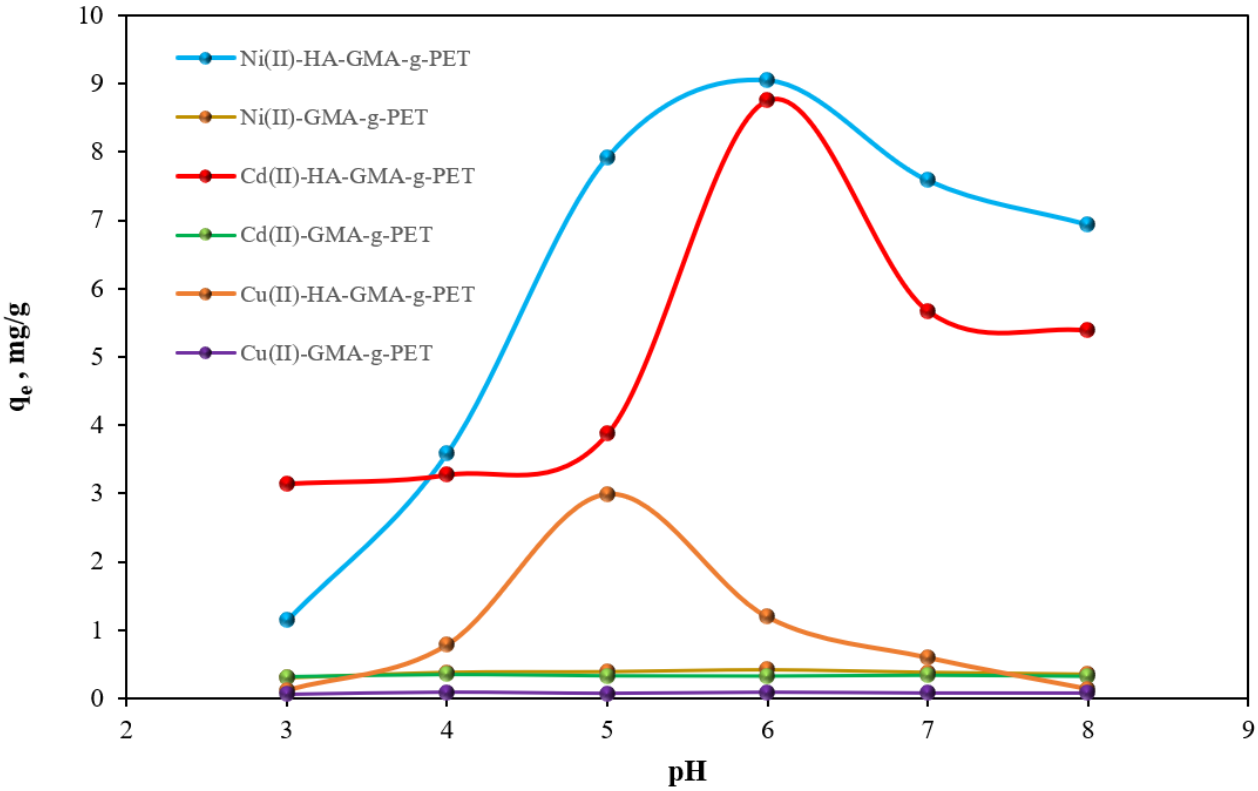

Figure 6: Effect of pH on the adsorption of Cu(II), Ni(II), and Cd(II) ions on HA-GMA-g-PET fibers (25 °C, 120 min, grafting yield, 95%).

3.4. Effect of Contact Time

We examined how adsorption time affects the adsorption of metal ions from an aqueous solution of HA-functionalized GMA-g-PET fiber using the batch method, and the results are shown in Figure 7. The adsorption process is highly dependent on the ion

exchange of the grafted modified polymer, its chelation properties, the openness of the binding sites of the polymer to the interaction surface, and the degree of diffusion of the analyte cations (17). When the figure is examined, it can be seen that adsorption occurs rapidly at first. The abundance of active binding sites on the surface of HA-GMA-g-PET fibers can initially explain the reason for this. As time progresses, active binding sites gradually decrease and equilibrium is reached. Cu(II), Ni(II), and Cd(II) ions reached the maximum adsorption value after 90, 45, and 120 min, respectively.

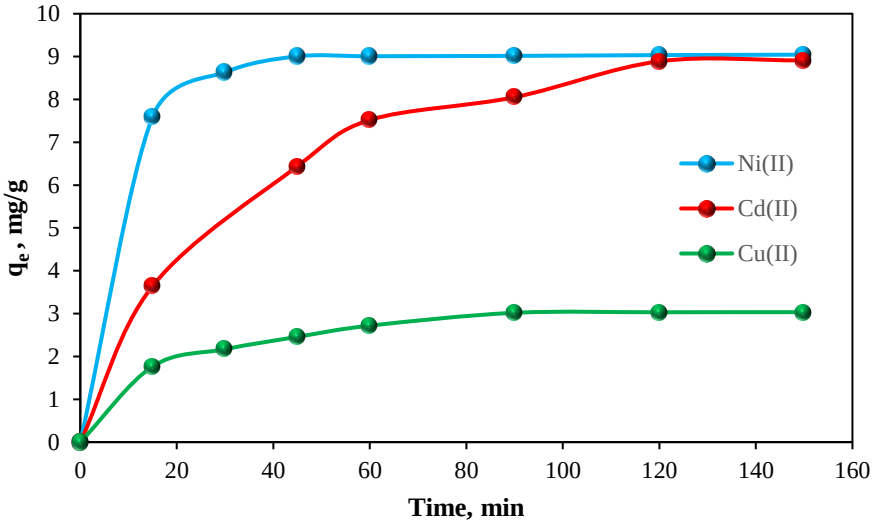

Figure 7: Effect of the contact time on the adsorption of Cu(II), Ni(II), and Cd(II) ions on HA-GMA-g-PET fibers (Analyte concentrations, 20 mg/L; 25 °C; grafting yield, 95%; pH 5 for Cu(II), 6 for Ni(II) and Cd(II)).

To investigate the adsorption mechanism, the pseudo-first-order model (PFO) and pseudo-second-order model (PSO) were used to test dynamic experimental data. The linearized equation of the pseudo-first-order model proposed by Lagergren (17) is given in equation (4):

$$Log(q_e - q_t) = Log q_e - (\frac{k_1}{2.303})t \quad (4)$$

In this context, qt represents the amount of ions adsorbed at any time (in mg of ions adsorbed per gram of adsorbent), qe denotes the amount of substance adsorbed at equilibrium, and k_1 indicates the rate constant (in min^{-1}). According to the equation, the log(q_e-q_t) versus t (Figure 8) graph was drawn, and the k_1 value was calculated from the slope of the line. The theoretical amount of adsorbed substance, q_e, was calculated from the intersection point of the theoretical line, and the results are shown in Table 1.

The linearized form of the pseudo-second-order model developed by Ho and McKay (18) is given in equation (5):

$$\frac{t}{q_t} = \frac{1}{k_2 q_e^{\,2}} + \frac{t}{q_e} \quad (5)$$

Where k_2 (g/mg/min) is the rate constant (PSO), q_e is calculated from the slope of the line obtained from the graph drawn with t values against t/q_t, k_2 is calculated from the theoretical and cut points, and the results are shown in Table 1.

Table 1: PFO and PSO rate constants.

Metal	$q_{e,\,exp}$ (mg/g)	PFO rate constants			PSO rate constants		
		k_1 (min^{-1})	$q_{e,\,cal}$ (mg/g)	R^2	k_2 (g/mg/min)	$q_{e,\,cal}$ (mg/g)	R^2
Cu(II)	3.03	0.0306	2.10	0.987	0.0209	3.31	0.994
Ni(II)	9.03	0.1216	10.25	0.977	0.0412	9.34	0.995
Cd(II)	8.89	0.0251	6.70	0.978	0.0032	10.74	0.995

When Table 1 is examined, the regression numbers of the lines drawn from the second-order velocity equation are greater than the regression numbers of the lines drawn from the first-order velocity equation. In addition, the theoretical q values calculated from the second-order velocity equation showed better agreement with the experimental q values (Figure 9). The data obtained showed compliance with the second-order adsorption mechanism.

3.5. Effects of Temperature on Adsorption

The effect of temperature on the adsorption of metal ions from aqueous solution by HA-functionalized GMA-g-PET fibers was investigated. As seen in Figure 10, there was a slight increase in the amount of adsorption with the increase in temperature. As the temperature increased, the swelling percentage of the fiber increased. Thus the amount of adsorbed metal ions increased as the diffusion of metal ions into the grafted fibers became easier.

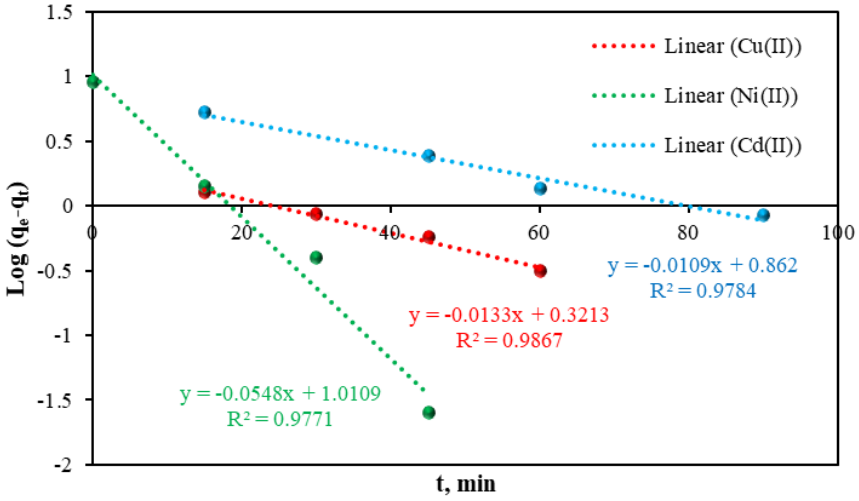

Figure 8: Pseudofirst-order plots for Cu(II), Ni(II) and Cd(II) ions on HA-GMA-g-PET fiber.

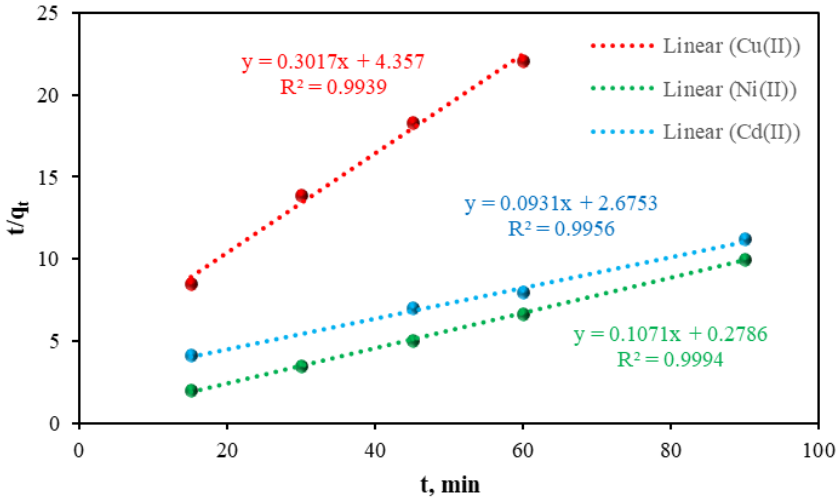

Figure 9: Pseudo-second-order plots for Cu(II), Ni(II) and Cd(II) ions on HA-GMA-g-PET fibers.

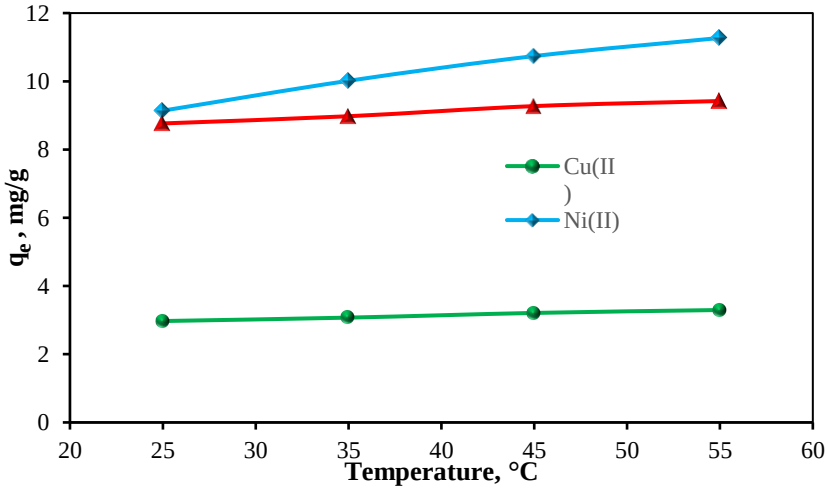

Figure 10: Effect of temperature on the adsorption of Cu(II), Ni(II), and Cd(II) ions on HA-GMA-g-PET fibers (Analyte concentrations, 20 mg/L; grafting yield, 95%; pH 5 for Cu(II), 6 for Ni(II) and Cd(II)).

The 1/T plot against Log q values for Cu(II), Ni(II), and Cd(II) ions is shown in Figure 11. From the slopes of the lines, the adsorption energies of the adsorption of Cu(II), Ni(II), and Cd(II) ions were calculated as 0.345, 0.685, and 0.244 kJ mol^{-1}, respectively. The activation energy required for chemical adsorption has been reported in the range of 65-250 kJ/mol (19). The fact that the obtained values are significantly lower than this range indicates physical adsorption. Low activation energies showed that the adsorption of metal ions by HA-GMA-g-PET fibers occurred easily.

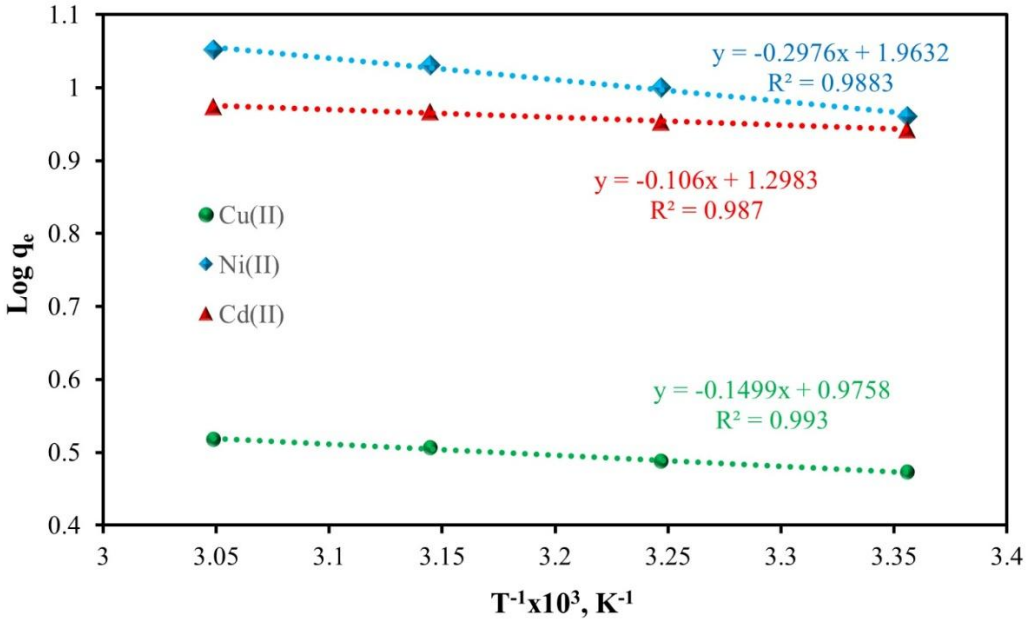

Figure 11: Log q value versus 1/T plot for Cu(II), Ni(II), and Cd(II) ions.

3.6. Effect of Initial Ion Concentration

Figure 12 shows the effect of the initial concentration of Cu(II), Ni(II), and Cd(II) ions on the adsorption on HA-GMA-g-PET fibers under optimum conditions. It was observed that the adsorption of Cu(II) ions remained almost constant after the initial concentration of 200 mg/L, and the adsorption of Ni(II) and Cd(II) ions remained almost constant after the initial concentration of 300 mg/L. The maximum adsorption capacities for 300 mg/L Cu(II), Ni(II), and Cd(II) were obtained as 27.76, 63.86, and 66.73 mg/g, respectively. The results indicate that the affinity of Ni(II) and Cd(II) ions is higher than that of Cu(II) for HA-GMA-g-PET fibers.

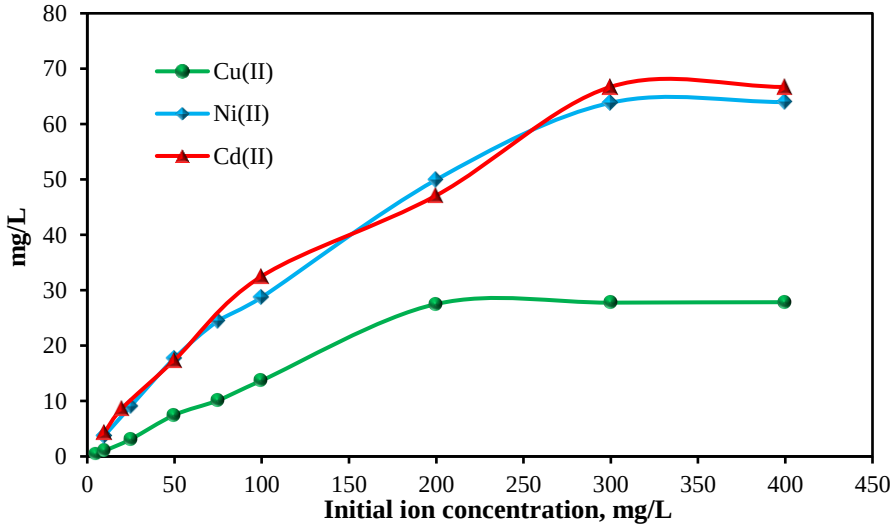

Figure 12: Effect of ion initial concentration on the adsorption of Cu(II), Ni(II), and Cd(II) ions onto HA-GMA-g-PET fibers (Time: 120 min; temperature: 25 °C; adsorbent concentration: 0.05 g/0.025 L; grafting yield: 95%; pH 5 for Cu(II), 6 for Ni(II) and Cd(II)).

The literature reports the adsorption capacities of various adsorbents for heavy metal ions as follows: 0.129-21.40 mg/g for Cu(II) ion, 0.069-13.90 mg/g for Ni(II) ion, and 0.112-48.80 mg/g for Cd(II) ion. It has been reported to be in the range of (20-25). Accordingly, it is thought that the adsorption capacity of HA-GMA-g-PET fiber is quite satisfactory for Cd(II) and Ni(II) ions, and at the level of adsorbents given in the literature for Cu(II) ions.

It has been found that HA-GMA-g-PET fiber has a beneficial adsorbent feature in the selective removal of Cd(II) ions, which are highly toxic, from aqueous solution, and it removes Ni(II) and Cu(II) ions at the level of adsorbents given in the literature. According to these results, it is thought that HA-GMA-g-PET fibers can be used as an alternative industrial adsorbent.

3.7. Adsorption Isotherm

The amount of a chemical species adsorbed by an adsorbent is expressed by adsorption isotherms, which relate a function to the equilibrium concentration of the species of interest at constant temperature. Adsorption isotherm models provide information about adsorption mechanisms and affinities (25,26). In this study, Langmuir (27) and Freundlich (28) isotherms, which are the most preferred in the literature, were used.

The linearized equations of the Langmuir and Freundlich isotherms are given in equations 6 and 7, respectively.

$$\frac{Ce}{Qe} = \frac{1}{Q_m k_L} + \frac{Ce}{Q_m} \quad (6)$$

$$LogQe = LogK_F + \frac{1}{n} LogCe \quad (7)$$

where C_e is the concentration of Cu(II), Ni(II), and Cd(II) ions (mg/L) at equilibrium. Q_e is the amount of substance adsorbed on the unit adsorbent (mg/g), Q_m indicates the monolayer adsorption capacity of the adsorbent (mg/g), and K_L is the Langmuir adsorption constant (L/mg). K_F and n refer to adsorption capacity (mg/g) and empirical parameter, respectively.

According to the Langmuir equation, the C_e/q_e versus C_e graph was drawn as shown in Figure 13, q_m values were calculated from the slope of the line, and K_L values were calculated from the intersection, and the results are given in Table 2.

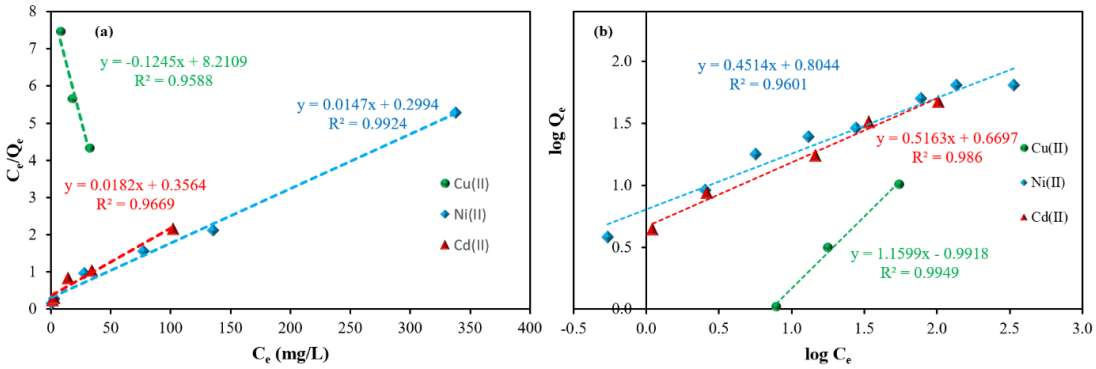

Figure 13: Linear fit curves for (a) Langmuir and (b) Freundlich adsorption isotherm models.

According to the regression coefficients of the isotherms, it can be said that the Freundlich isotherm for Cu(II) and Cd(II) and the Langmuir isotherm for Ni(II) better describe the adsorption mechanism of these ions on HA-GMA-g-PET fiber. It indicates the single-layer adsorption of Ni(II) ions on homogeneously distributed adsorption sites of HA-GMA-g-PET fibers and the multilayer adsorption of Cu(II) and Cd(II) ions on heterogeneous adsorption sites. The value of 1/n<1 obtained for Ni(II) and Cd(II) indicates the strong adsorption bond within the adsorbent layers, while there is a weak adsorption bond for Ni(II). The Q_m for Cu(II), Ni(II), and Cd(II) ions were 8.03, 68.02, and 54.94 mg/g, respectively.

Table 2: Freundlich and Langmuir isotherm constants.

Metal	Freundlich constant			Langmuir constant		
	K_F	n	R^2	Q_m (mg/g)	K_L (L/mg)	R^2
Cu	0.12	0.86	0.995	8.03	1.02	0.960
Ni	6.37	2.21	0.960	68.02	0.004	0.993
Cd	4.67	1.93	0.986	54.94	0.006	0.966

3.8. Selective Adsorption of Metal Ions

We examined the use of HA-GMA-g-PET fibers as adsorbents for selective adsorption in aqueous solutions containing binary and ternary mixtures of metal ions. The results of the removal of metal ions by HA-GMA-g-PET fiber from equimolar solutions of Cu(II), Ni(II), and Cd(II) ions at optimum pH value are shown in Figure 14. Cu(II)-Cd(II) (Figure 14a), Ni(II)-Cd(II) (Figure 14b), and Cu(II)-Ni(II)-Cd(II) (Figure 14c) are examples of binary and triplet. In the mixtures, Cd(II) ions showed better affinity to HA-GMA-g-PET fiber, and adsorption selectivity was achieved at 85%. This indicates that it will allow the selective separation of Cd(II) ions in aqueous samples containing Cu(II) and Ni(II) ions.

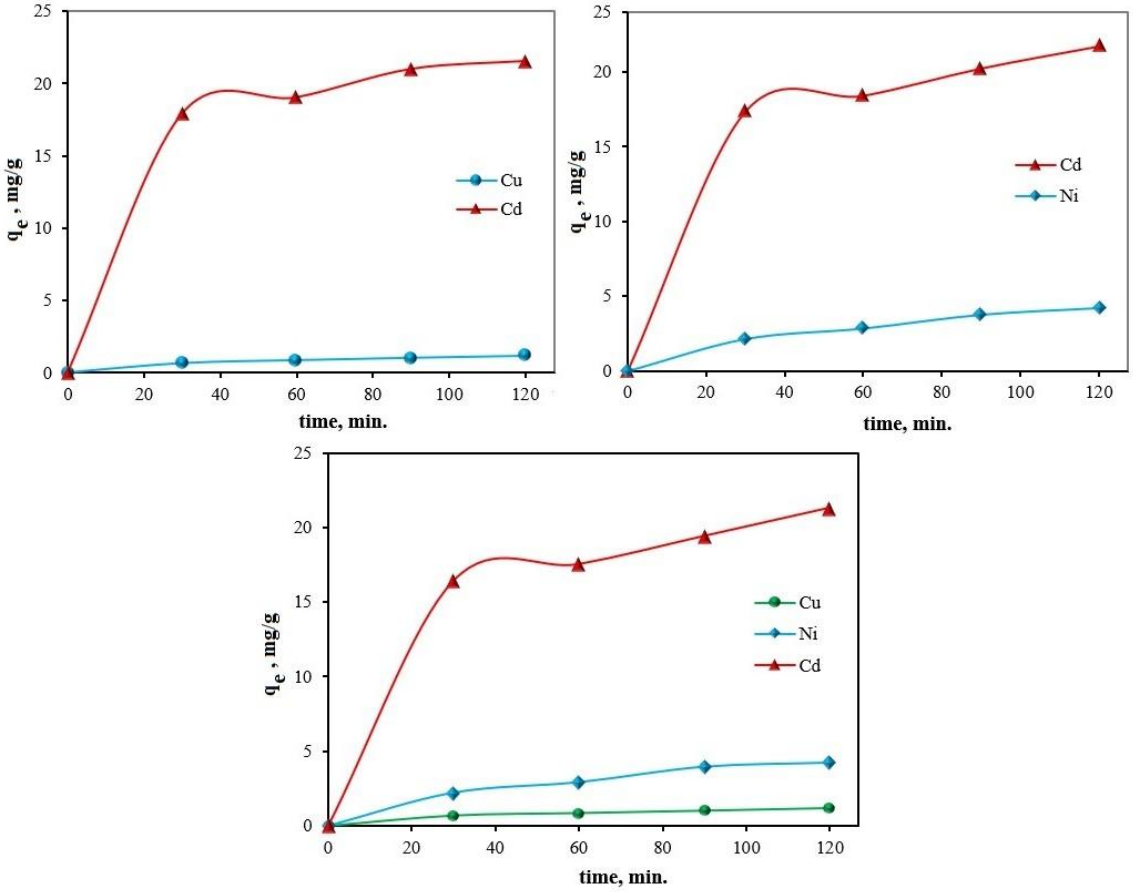

Figure 14: The process involves the competitive adsorption of ions onto HA-GMA-g-PET fibers. [(a) Cd(II)–Cu(II); (b) Cd(II)–Ni(II); (c) Cd(II)–Cu(II)–Ni(II); pH 6; ion concentration: 50 mg/L; contact time: 120 min; temperature = 25 °C; graft yield: 95%]

3.9. Desorption of Metal Ions

We examined the desorption properties of Cu(II), Ni(II), and Cd(II) ions adsorbed on HA-GMA-g-PET fiber. The results obtained were shown in Figure 15. Adsorbed metal ions were easily desorbed with 25 mL of 1 mol/L HNO_3 in 60 minutes at room temperature. The highest desorption values for Cu(II), Ni(II), and Cd(II) ions were found to be 99%, 99%, and 98%, respectively. The desorption of metal ions was rapid and completed in a short time. The high and rapid desorption rate supported the proposed adsorption mechanism. These desorption results indicate that HA-GMA-g-PET fibers can be used in industrial applications as an effective adsorbent in removing the studied metal ions from wastewater.

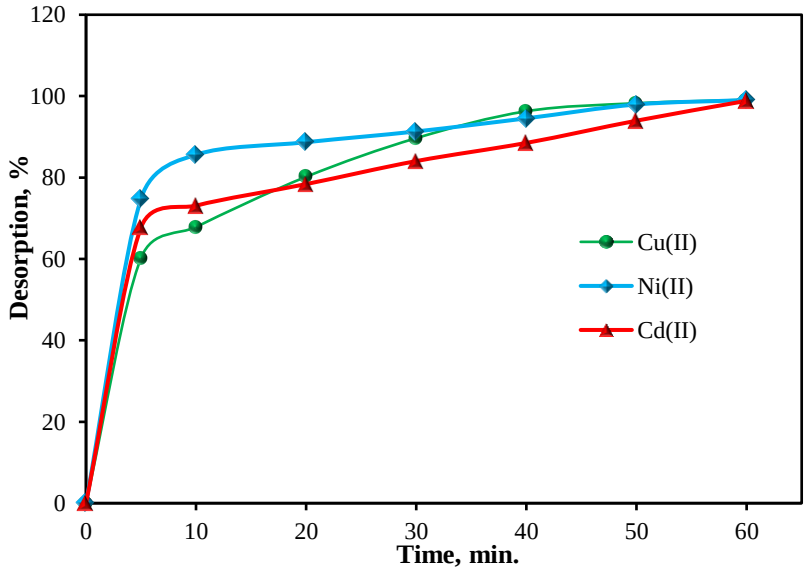

Figure 15: Desorption profile of HA-GMA-g-PET fibers with adsorbed Cu(II), Ni(II), and Cd(II) ions. (Graft yield: 95%; ions concentration: 50 mg/L; temperature: 25°C; contact time: 60 min.)

The desorption of metal ions was rapid and completed in a short time. The high and rapid desorption rate supported the proposed adsorption mechanism. These desorption results indicate that HA-GMA-g-PET fibers can be used in industrial applications as an effective adsorbent in removing the studied metal ions from wastewater.

3.10. Reusability of HA-GMA-g-PET Fibers

One of the most important features of an effective and economical adsorbent is that it can be used repeatedly. We investigated how the repeated use of HA-GMA-g-PET fiber as an adsorbent affects the adsorption of Cd(II) ion. For this purpose, the adsorption and desorption process was repeated five times, and the results are shown in Figure 16. It was observed that there was an approximately 9% decrease in the amount of Cd(II) metal ion adsorbed after five repetitions. The results indicate that HA-GMA-g-PET fibers can be used as a suitable adsorbent with high reusability in the adsorption of Cd(II) ions.

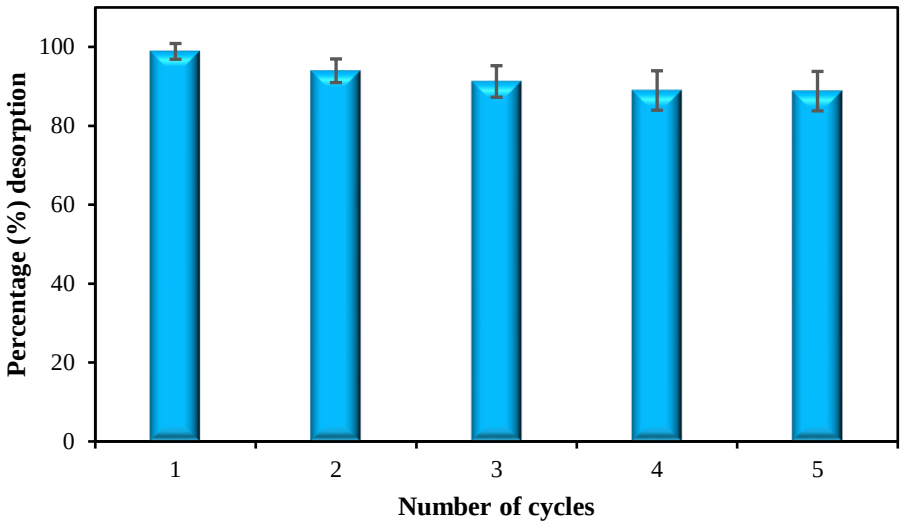

Figure 16: Adsorption–desorption of Cd(II) ions and reusability of adsorbent using HNO_3 as desorbing agent (n:3). (Graft yield: 95%; pH 6; Cd(II) ions concentration: 50 mg/L; temperature: 25°C; contact time: 120 min.)

4. CONCLUSION

GMA monomers were grafted onto PET fibers in an aqueous medium using a benzoyl peroxide initiator. The GMA-g-PET fiber was treated with HA, studied to understand its properties, and tested to see how well it can remove heavy metal ions. It was noticed that factors like temperature, how long the reaction takes, and how well the GMA-impregnated PET fiber is soaked with HA influence how well the fiber is functionalized. It was observed that various parameters, such as pH, adsorption time, adsorption temperature, and initial ion concentration, affect the adsorption capacity of Cu(II), Ni(II), and Cd(II) ions on HA-GMA-g-PET fibers. It was found that the maximum adsorption of Cu(II) ions occurred at pH 5, while Ni(II) and Cd(II) ions reached maximum adsorption at pH 6 on HA-GMA-g-PET fibers. The Cu(II), Ni(II), and Cd(II) ions quickly attached to the HA-GMA-g-PET fibers in the first 30 minutes, with Cu(II) ions stabilizing after 90 min, Ni(II) ions after 45 min, and Cd(II) ions after 120 min. It was found that the way Cu(II), Ni(II), and Cd(II) ions attach to HA-GMA-g-PET fibers followed a pattern described by a second-order kinetic model. The adsorption of Cu(II), Ni(II), and Cd(II) ions onto HA-GMA-g-PET fibers increased with the initial ion concentration, and the maximum adsorption amounts of Cu(II), Ni(II), and Cd(II) ions were found to be 27.76 mg/g, 63.86 mg/g, and 66.73 mg/g, respectively. The adsorption of heavy metal ions onto HA-GMA-g-PET fibers follows the Freundlich adsorption isotherm for Cu(II) and Cd(II) ions and the Langmuir adsorption isotherm for Ni(II) ions. The Cu(II), Ni(II), and Cd(II) ions stuck to HA-GMA-g-PET fibers were removed at a rate of 98% using a 1 mol/L HNO_3 solution. It was discovered that Cd(II) ions were taken out more efficiently, at a rate of 85%, from mixtures that included Cu(II) and Cd(II) or Ni(II) and Cd(II), as well as from a mixture of Cu(II), Ni(II), and Cd(II). The HA-GMA-g-PET fiber was subjected to five adsorption and desorption cycles for reuse. After five reuses, the amount of adsorbed metal ions decreased by 9%. The adsorbent's selectivity toward Cd(II) ions, which are highly toxic, is an important property. Due to its reusability, the synthesized material is anticipated to serve as an alternative adsorbent.

5. CONFLICT OF INTEREST

The authors assert that they possess no recognized competing financial interests or personal relationships that may have influenced the work presented in this paper.

6. REFERENCES

1. Wang LJ, Tian ZB, Li H, Cai J, Wang SJ. Spatial and temporal variations of heavy metal pollution in sediments of Daning River under the scheduling of three gorges reservoir. In: Proceedings of the 2016 International Forum on Energy, Environment and Sustainable Development [Internet]. Atlantis Press;

2016. p. 1036–47. Available from: <URL>.

2. Wanj J, Zhang YM, Xu M, Liu BQ. Heavy metal pollution of surface sediments in the northern waters of the abandoned Yellow River Delta in Jiangsu Province of China and ecological risk assessment. Appl Ecol Environ Res [Internet]. 2019;17(6):14867–82. Available from: <URL>.

3. Maal-Bared R. Operational impacts of heavy metals on activated sludge systems: The need for improved monitoring. Environ Monit Assess [Internet]. 2020 Sep 3;192(9):560. Available from: <URL>.

4. Hashim ESH, Al-Yassein RN. Effect of sublethal concentrations of cadmium on the histo-pathological changes of muscles of planiliza abu juveniles (Heckel, 1843). Basrah J Agric Sci [Internet]. 2020 Nov 13;33(2):207–17. Available from: <URL>.

5. Zhou X, Wang YP, Song Z. Heavy metal contamination and ecological risk assessments in urban mangrove sediments in Zhanjiang Bay, South China. ACS Omega [Internet]. 2022 Jun 21;7(24):21306–16. Available from: <URL>.

6. Lu R, Rong S, Wu J, Yue W, Li Q. Pollution assessment and SSD-based ecological assessment of heavy metals in multimedia in the coast of Southeast China. Int J Environ Res Public Health [Internet]. 2022 Nov 30;19(23):16022. Available from: <URL>.

7. Amor C, Marchão L, Lucas MS, Peres JA. Application of advanced oxidation processes for the treatment of recalcitrant agro-industrial wastewater: A review. Water [Internet]. 2019 Jan 25;11(2):205. Available from: <URL>.

8. Ayob S, Othman N, Hamood Altowayti WA, Khalid F, Bakar N, Tahir M, et al. A review on adsorption of heavy metals from wood-industrial wastewater by oil palm waste. J Ecol Eng [Internet]. 2021 Mar 1;22(3):249–65. Available from: <URL>.

9. Sen TK. Agricultural solid wastes based adsorbent materials in the remediation of heavy metal ions from water and wastewater by adsorption: A review. Molecules [Internet]. 2023 Jul 21;28(14):5575. Available from: <URL>.

10. Arslan M. Use of 1,6-diaminohexane-functionalized glycidyl methacrylate-g-poly(ethylene terephthalate) fiber for removal of acidic dye from aqueous solution. Fibers Polym [Internet]. 2010 Apr 5;11(2):177–84. Available from: <URL>.

11. Ioakeimidis C, Fotopoulou KN, Karapanagioti HK, Geraga M, Zeri C, Papathanassiou E, et al. The degradation potential of PET bottles in the marine environment: An ATR-FTIR based approach. Sci Rep [Internet]. 2016 Mar 22;6(1):23501. Available from: <URL>.

12. Sepperumal U, Markandan M, Palraja I. Micromorphological and chemical changes during biodegradation of Polyethylene terephthalate (PET) by Penicillium sp. J Microbiol Biotechnol Res Sch Res Libr J Microbiol Biotech Res [Internet]. 2013;3(4):47–53. Available from: <URL>.

13. Bozkaya O, Günay K, Arslan M, Gün Gök Z. Removal of anionic dyes with glycidyl methacrylate-grafted polyethylene terephthalate (PET) fibers modified with ethylenediamine. Res Chem Intermed [Internet]. 2021 May 21;47(5):2075–93. Available from: <URL>.

14. Yu X, Tong S, Ge M, Wu L, Zuo J, Cao C, et al. Synthesis and characterization of multi-amino-functionalized cellulose for arsenic adsorption. Carbohydr Polym [Internet]. 2013 Jan 30;92(1):380–7. Available from: <URL>.

15. Gün Gök Z, Günay K, Arslan M, Yiğitoğlu M. Removing of Congo red from aqueous solution by 2-hydroxyethyl methacrylate-g-poly(ethylene terephthalate) fibers. Polym Bull [Internet]. 2019 Dec 14;76(12):6179–91. Available from: <URL>.

16. Kumar R, Sharma RK, Singh AP. Grafting of cellulose with N-isopropylacrylamide and glycidyl methacrylate for efficient removal of Ni(II), Cu(II) and Pd(II) ions from aqueous solution. Sep Purif Technol [Internet]. 2019 Jul 15;219:249–59. Available from: <URL>.

17. Kalyani S, Priya JA, Rao PS, Krishnaiah A. Removal of copper and nickel from aqueous solutions using chitosan coated on perlite as biosorbent. Sep Sci Technol [Internet]. 2005 May;40(7):1483–95. Available from: <URL>.

18. Ho Y., McKay G. Pseudo-second order model for sorption processes. Process Biochem [Internet]. 1999 Jul 1;34(5):451–65. Available from: <URL>.

19. Yi-Yong C, Xing-Zhong Y. Synthesis and properties of 1-(2-aminoethyl)piperazine resin used in the sorption of the platinum group and gold ions. React Polym [Internet]. 1994 Oct 1;23(2–3):165–72. Available from: <URL>.

20. Wang S, Kwak JH, Islam MS, Naeth MA, Gamal El-Din M, Chang SX. Biochar surface complexation and Ni(II), Cu(II), and Cd(II) adsorption in aqueous solutions depend on feedstock type. Sci Total Environ [Internet]. 2020 Apr 10;712:136538. Available from: <URL>.

21. Hassan M, Naidu R, Du J, Qi F, Ahsan MA, Liu Y. Magnetic responsive mesoporous alginate/β-cyclodextrin polymer beads enhance selectivity and adsorption of heavy metal ions. Int J Biol Macromol [Internet]. 2022 May 15;207:826–40. Available from: <URL>.

22. Senila M, Neag E, Cadar O, Kovacs ED, Aschilean I, Kovacs MH. Simultaneous removal of heavy metals (Cu, Cd, Cr, Ni, Zn and Pb) from aqueous solutions using thermally treated romanian zeolitic volcanic tuff. Molecules [Internet]. 2022 Jun 20;27(12):3938. Available from: <URL>.

23. Han F, Zong Y, Jassby D, Wang J, Tian J. The interactions and adsorption mechanisms of ternary heavy metals on boron nitride. Environ Res [Internet]. 2020 Apr 1;183:109240. Available from: <URL>.

24. Annou B, Lebkiri I, Ouaddari H, Kadiri L, Ouass A, Habsaoui A, et al. Removal of Cd(II), Cu(II), and Pb(II) by adsorption onto natural clay: A kinetic and thermodynamic study. Turkish J Chem [Internet]. 2021 Apr 28;45(2):362–76. Available from: <URL>.

25. Hassan M, Liu Y, Naidu R, Du J, Qi F, Donne SW, et al. Mesoporous biopolymer architecture enhanced the adsorption and selectivity of aqueous heavy-metal ions. ACS Omega [Internet]. 2021 Jun 15;6(23):15316–31. Available from: <URL>.

26. Al-Ghouti MA, Da'ana DA. Guidelines for the use and interpretation of adsorption isotherm models: A review. J Hazard Mater [Internet]. 2020 Jul;393:122383. Available from: <URL>.

27. Langmuir I. The adsorption of gases on plane surfaces of glass, mica and platinum. J Am Chem Soc [Internet]. 1918 Sep 1;40(9):1361–403. Available from: <URL>.

28. Freundlich H. Über die adsorption in lösungen. Zeitschrift für Phys Chemie [Internet]. 1907 Oct 1;57U(1):385–470. Available from: <URL>.